The Pennsylvania State University

The Graduate School

College of Earth and Mineral Sciences

PREDICTABILITY AND DYNAMICS OF A NON-INTENSIFYING TROPICAL STORM: ERIKA (2009)

A Thesis in

Meteorology

by

Erin B. Munsell

Submitted in Partial Fulfillment
of the Requirements
for the degree of

Master of Science

December 2012

The thesis of Erin B. Munsell was reviewed and approved* by the following:

Fuqing Zhang
Professor of Meteorology
E. Willard and Ruby S. Miller Faculty Fellow
Joint Appointment with the Department of Statistics
Thesis Adviser

Jenni L. Evans
Professor of Meteorology

Marcelo Chamecki
Assistant Professor of Meteorology

Johannes Verlinde
Professor of Meteorology
Associate Head, Graduate Program in Meteorology

*Signatures are on file at the Graduate School

Abstract

In this study, the predictability of Tropical Storm Erika (2009) is evaluated by analyzing a 60-member convection-permitting ensemble initialized with perturbations from a real-time Ensemble Kalman Filter (EnKF) system. Erika was forecast to intensify into a hurricane by most operational numerical models, but in reality never exceeded 50 kts. There is a fairly large spread in the final intensities of the 60 ensemble members indicating large uncertainty in the deterministic prediction of Erika's intensity at 36-48-h lead times. An investigation into which factors prevented intensification of the weaker ensemble members provides insight that may aid in the forecasting of the intensity of future tropical cyclones under similar conditions.

A variety of environmental and storm-related factors are examined, and the parameters that have the greatest relation to future intensity are determined based on ensemble sensitivity and correlation analysis. It appears that mid-level relative humidity, absolute vorticity, and the distribution of convection relative to the storm center all play a role in determining whether a given ensemble member intensifies or not. In addition, although differences in deep-layer shear among ensemble members are difficult to discern, many of the ensemble members that do not intensify fail to do so because of apparent dry air intrusions that wrap around the centers of the storms, particularly in the 700-500 hPa layer. In the presence of moderate shear, this dry air is able to penetrate the cores of the cyclones, thereby preventing further development.

Table of Contents

List of Figures

(black circles) for the members of the composite groups 8WEAKEST and 8STRONGEST. Three of the members in the 8WEAKEST group do not have distinguishable circulation centers at forecast hour 42 and therefore are not plotted.

Acknowledgements:

The author wishes to thank her advisor, Fuqing Zhang, and the members of her committee, Jenni Evans and Marcelo Chamecki, for their insightful comments and suggestions. A special thanks to Daniel Stern for his unwavering support and guidance and to Yonghui Weng for performing all of the ensemble simulations of Tropical Storm Erika. This research is partially supported by NSF Grant 0840651, Office of Naval Research Grant N000140910526 and the NOAA Hurricane Forecast Improvement Project (HFIP).

CHAPTER 1: Introduction

Significant advances have been made over the past few decades in the skill of hurricane track forecasts (Rappaport et al. 2009). However, the skill of intensity prediction has not improved at a rate anywhere near that of the track forecasts (Elsberry et al. 2007; DeMaria et al. 2005). More recent studies focus on the processes and environmental conditions that lead to genesis and rapid intensification, which are important to intensity forecasts. In contrast, this study investigates the predictability of the intensification (or lack thereof) of a weak tropical cyclone that has already undergone genesis. Tropical Storm Erika (2009) originated from a westward moving tropical wave that emerged into the Atlantic Ocean off the western coast of Africa on 25 August 2009 (Berg and Avila 2011). Shower and thunderstorm activity began to increase on 27 August 2009 as a broad area of low pressure formed. On 29 August 2009, as the wave tracked westward south of the Cape Verde Islands, convection began to diminish. However, on 30 August 2009, the wave encountered a region of warmer sea surface temperatures and convection began to redevelop. At this time, scatterometer data indicated that the storm had tropical storm force winds but lacked a well-defined low-level circulation center. By the next day, satellite imagery indicated that the storm had become better defined and a United States Air Force Reserve reconnaissance aircraft identified a broad, but closed, circulation about 250 nautical miles (n mi) east of Guadeloupe. Therefore, Tropical Storm Erika was officially designated on 1800 UTC 1 September 2009 with a minimum sea level pressure (SLP) of 1007 hPa and maximum sustained winds of 45 kts (Berg and Avila 2011). Even though the wave was upgraded to a tropical storm, the circulation was exposed, and a large cluster of thunderstorms was located well east of the surface center of the storm (Fig. 1a). Over the next few days, Erika struggled to intensify (Fig. 1). The magnitude of the AMSU deep-layer wind shear (Zehr et al.

2008) was initially strong (30 kts) but quickly decreased to a more modest value, ranging between 5 kts and 20 kts (to be shown later). In addition, the shear was from the southwest throughout the lifetime of the storm, which is consistent with the deep convection associated with Erika remaining to the northeast (downshear) and displaced from the circulation center. Forecasters at the National Hurricane Center (NHC) believed that this southwesterly shear played a significant role in preventing the convection from becoming more organized and wrapping around the circulation center, and therefore contributed to the lack of strengthening of Tropical Storm Erika.

Erika continued moving westward, weakening to a minimal tropical storm (maximum sustained winds of 35 kts), as the circulation center passed over Guadeloupe at approximately 1800 UTC 2 September 2009. Early on 3 September 2009, thunderstorm activity slightly increased and the storm began to reintensify (to 40 kts at 0600 UTC 3 September 2009). This increase in convection is evident in Fig. 1e (1145 UTC 3 September 2009) as the convection increases in areal coverage, although it remains displaced from the circulation center. This intensification period was brief however, and Erika was downgraded to a tropical depression at 1800 UTC 3 September 2009, and further weakened to a remnant low 6 hours later as it passed to the south of Puerto Rico. Tropical Storm Erika reached its peak intensity at 0000 UTC 2 September 2009 with a minimum SLP of 1004 hPa and maximum sustained winds of 45 kts.

The genesis of Erika was very well forecasted (Berg and Avila 2011; Brown 2009). However, nearly all operational intensity models forecasted the tropical storm to intensify into a hurricane although the storm failed to do so. The official NHC forecast did not intensify Erika into a hurricane, however significant intensity errors were still seen (Brown 2009). Utilizing the methodology employed in previous predictability studies (Zhang and Sippel 2009; Sippel and

Zhang 2010), a 60-member WRF ensemble simulation of Tropical Storm Erika is performed and analyzed in an attempt to identify which environmental and internal factors contributed to the lack of intensification of this storm. An understanding of what processes prevented the weak ensemble members from intensifying may help to understand why this lack of intensification for Erika was difficult to forecast and more generally, increase the understanding of the predictability of weaker tropical systems.

Section 2 describes the model and ensemble set-up used for the simulations, as well as the statistical tools used to analyze the output of this simulation. Section 3 discusses the overall performance of the simulation and explains in detail how differences in the environmental factors among the ensemble contribute to the spread in final intensity. Finally, Section 4 summarizes the main conclusions of this study.

CHAPTER 2: Research Methodology

Model Description and Ensemble Analysis

In this study a 60-member cloud-permitting ensemble using the advanced research version (ARW) of the Weather Research and Forecasting (WRF) model version 3.1.1 (Skamarock et al. 2008) is performed and analyzed. Two static, two-way nested domains are used for all ensemble members with horizontal grid spacings of 13.5 km and 4.5 km, respectively, and 34 vertical levels. Each domain has 541 by 604 horizontal grid points, which correspond to areas covering approximately 7300 by 8100 km and 2400 by 2700 km respectively. The physics configurations are consistent with those used in Zhang et al. (2010). These include the Yonsei University (YSU) (Noh et al. 2003) planetary boundary layer parameterization scheme, and the WRF single-moment six-class (WSM6) microphysics parameterization scheme (Hong et al. 2004). There are no cumulus parameterizations used in either domain. The model is integrated from 0000 UTC 2 September 2009 until 0000 UTC 4 September 2009, which corresponds with the time from 6 hours after Erika was officially designated as a tropical storm until the time at which Erika was declared a remnant low. As in Zhang et al. (2010), the initial and boundary conditions of the 60 ensemble members are derived from ensemble perturbations generated by the real-time Global Forecast System (GFS)-EnKF global ensemble data assimilation system (Whitaker et al. 2008). This real-time GFS-EnKF system (Whitaker et al. 2008) uses the same GFS model and assimilates the same set of observations as those in the NCEP operational GSI analysis. This system has demonstrated advantages over the NCEP then-operational system due to its use of a more advanced data assimilation technique (Hamill et al. 2011). The ensemble perturbations derived from the GFS-EnKF analysis and forecast system thus represent realistic uncertainties in the initial and

boundary conditions for the ensemble prediction of Erika, which eventually lead to large ensemble spread in the 48-h forecast of intensity.

Correlation Analyses

To assess environmental and storm-related factors that affect the predictability of Erika, a correlation analysis based on ensemble sensitivity is performed. As in previous predictability studies (e.g., Sippel and Zhang 2008, 2010; Sippel et al. 2011) correlation thresholds of 'weak', 'moderate' and 'strong' are chosen to be 0.3, 0.5, and 0.7 respectively[1]. Throughout this study, correlations are calculated between a given factor and the final intensities of the ensemble, in order to assess the impact of that factor on the intensity spread of the ensemble. The metric used for "final" intensity is the minimum SLP of each ensemble member forty-two hours into the simulation (forecast hour 42 or 1800 UTC 3 September 2009). The results of the correlation analysis corresponding to the time interval between forecast hour 12 and 24 are most relevant to identifying whether an ensemble member will intensify or not. This is the portion of the simulation after the WRF model "spin-up" (since the initial conditions are derived from a coarse resolution global model) has been completed but for which the intensities of the ensemble members are still similar to each other. As we will show, the influence of environmental and storm-related factors on the final intensity is strongest during this portion of the simulation (before some of the ensemble members have begun to intensify) and the analysis of the statistical correlations will therefore be focused on this 12-h period.

Although linear correlation is a valuable statistical tool, it is important to remember its limitations. First, correlation does not imply causation, and second, the variables could still be nonlinearly related even if they have little or no linear correlation. Furthermore, many of the

[1] Note that the thresholds in the current study will be more statistically significant than those in Sippel and Zhang (2008, 2010) with the doubling of the ensemble size from 30 to 60.

factors considered in this study that potentially influence the final intensity spread (atmospheric moisture, initial intensity, wind shear etc.) are correlated with each other. For example, as the simulation advances, the relative humidity becomes strongly correlated with current intensity, and so part of the correlation of humidity with final intensity is actually a consequence of the relationship between current and final intensity. Once the intensification process has begun for a given member, it is likely to continue unless significant changes occur in the surrounding environmental conditions. A simple linear correlation is insufficient when assessing relationships between the factors and the final intensities. Partial or "part" correlations are therefore used to clarify relationships when multiple variables are correlated to one another. A first-order partial correlation is equivalent to correlating variables x and y while holding z constant ($r_{y(x,z)}$). This first-order partial correlation is given by

$$r_{y(x,z)} = \frac{r_{yx} - r_{yz}r_{xz}}{\sqrt{1 - r_{xz}^2}}, \quad (1)$$

where r_{yx} is the correlation between variables x and y, r_{yz} is the correlation between y and z and r_{xz} is the correlation between x and z. Similar to Sippel et al. (2011), in all partial correlations calculated in this study the dependent variable y is the final intensity metric, z is the current intensity (current minimum sea level pressure) of each ensemble member and x is the factor that is being evaluated. Partial correlations are applied in an attempt to evaluate the relationship between the final intensity and the environmental and storm-related factors, while removing the impact that current intensity has on this relationship. Throughout this study, linear and partial correlations are the main statistical tools utilized in order to evaluate the impacts of a given factor on the intensity spread of these simulations.

CHAPTER 3: Results and Discussion

Ensemble Performance of Track and Intensity

An analysis of the tracks and intensities of the sixty ensemble members is performed to gain insight into whether the differences in ensemble tracks contributed to the significant spread in final intensity in any way. Figure 2a shows the NHC Best Track of Erika as well as the tracks of all sixty members in the ensemble grouped by final intensity. Erika tracked westward throughout its lifetime, and the Best Track lies along the southern edge of the area spanned by the ensemble tracks. Some of the ensemble members track generally westward, while others take a more northwestward heading. The NHC Tropical Cyclone report states that all operational models for this storm had a strong northward bias and unusually large track errors (Brown et al. 2009). The northward bias that exists in the ensemble tracks of this simulation was most likely caused by the same modeling errors that occurred in the track forecasts of the operational models. It appears that most of the more intense ensemble members travel in a more northwestward direction, while the weaker ensemble members can have either westward or northwestward tracks. However, the final position (in terms of latitude and longitude) and final intensity are only weakly correlated (not shown). This suggests that the tracks of the members may be influenced to some extent by their intensities but the track does not appear to contribute substantially to the intensity spread. The tracks of all ensemble members coincide with sufficiently high sea surface temperatures (SST, Fig. 2a) for further development (28°C -29°C), implying that SST also does not contribute to the intensity spread.

Figures 2b and 2c show a time evolution of the minimum SLP and maximum 10-m wind speed for each ensemble member, along with the Best Track intensity of Tropical Storm Erika. The initial intensities of the ensemble members are slightly weaker than the Best Track intensity

of Erika, perhaps due to the coarse (~47 km) resolution of the GFS-EnKF analyses, which provide the initial conditions. Given these similar initial intensities, Fig. 2 clearly illustrates that some ensemble members intensify while some do not. The black dashed line indicates the time that was chosen as a "final" intensity time when calculating statistical relationships (1800 UTC 3 September 2009). This time coincides with the operational downgrading of Tropical Storm Erika to Tropical Depression Erika. By the end of the simulation, the spread in intensity between the members is large. Overall, about half of the ensemble members (32) perform somewhat successfully by not appreciably intensifying, with a final minimum SLP greater than 1000 hPa. Another 19 members are considered to be average performers with final minimum SLPs between 990 hPa and 1000 hPa, while 9 ensemble members perform unsuccessfully and intensify to storms with minimum SLPs less than 990 hPa. These groups of ensemble members will be referred to as "WEAK", "AVERAGE" and "STRONG" throughout this study. During the first twelve hours of the simulation, spikes in intensity and unrealistic features in some of the environmental fields can be observed. These irregularities in intensity in the early part of the simulation can be clearly seen in the time evolution of the maximum wind speed of the ensemble members (Fig. 2c), as the maximum wind speeds of some members increase by as much as 40 kts. Presumably, these features result from the initial conditions being derived from a different model with coarser grid spacing, and so a period of adjustment must occur. Therefore, the statistical analysis of this study is focused on the times between 1200 UTC 2 September 2009 and 0000 UTC 4 September 2009.

The intensity evolution of four ensemble members is highlighted in Fig. 2 (Members 29, 25, 46 and 51), while Fig. 3 shows the time evolution of the 2-km simulated radar reflectivity fields that correspond with these four highlighted members. These members demonstrate the

diversity of the ensemble. Member 29 represents a typical weak member that has an average initial intensity among the other members of the ensemble, but fails to strengthen throughout the simulation. As the radar reflectivity fields indicate, there is little convection located near the circulation center of this storm throughout its lifetime. Member 25 fails to intensify to a minimum SLP less than 1000 hPa even though the member has one of the stronger initial intensities in the ensemble, and is representative of other such members. This implies that initial intensity does not completely determine whether a given member will intensify or not. There is also a larger areal coverage of convection associated with the initial vortex of this member and this convection may be a contributing factor in the evolution of the strength of the vortex. This member does begin to slowly intensify at 0000 UTC 3 September 2009 but later weakens at 1200 UTC 3 September 2009 when the strength of the convection weakens and becomes severely displaced from the circulation center.

Both members 46 and 51 intensify to minimum SLPs less than 990 hPa and are therefore two of the worst performing members in the ensemble. Member 46 is the strongest member in the ensemble, with a minimum SLP of 987 hPa at 1800 UTC 3 September 2009. A large area of strong convection in this member is initially located to the east of the circulation center. However, this convection is able to wrap around the low pressure center to form a closed eye by 1200 UTC 3 September 2009. The eye formation further accelerates the intensification process. Member 51 has the weakest initial intensity among all ensemble members but still does intensify. Once again, a large area of relatively strong convection remains close to the circulation center, which enables this member to intensify. Based on this preliminary analysis of four diverse ensemble members, it appears that the areal coverage, intensity and location of initial convection,

as well as the initial storm intensity, all play a role in determining which members intensify and which do not.

Factors Affecting Intensity

Atmospheric Moisture and Mid-level Dry-air Intrusions

Atmospheric moisture has long been recognized as an important environmental factor in the determination of tropical cyclone intensity. For example, Sippel and Zhang (2008), which utilized a similar ensemble set-up to this study, showed that the initial moisture profile of a member from the surface up to about 300-hPa has a moderate correlation with final intensity. The correlation between water vapor mixing ratio and final intensity in the mid-levels, particularly at 700-hPa, was shown to be strong. The presence of dry air in the mid-level portion of the atmospheric moisture profile can be particularly influential in preventing intensification from occurring. Dry air can wrap around a storm's core, and subsequently become entrained into the eyewall updrafts, which diminishes convection (Kimball 2006). In addition, lower equivalent potential temperatures in the mid-levels can correspond with cooler or drier air that can be advected to the boundary layer through evaporatively-induced downdrafts, weakening the storm (Reimer et al. 2010). Therefore, the atmospheric moisture profiles, specifically the relative humidity and equivalent potential temperature fields, are investigated to determine their impact on the intensity spread of the ensemble members in this simulation of Tropical Storm Erika.

Relative humidities at each vertical model level for each ensemble member are analyzed by finding the average relative humidity within a 200-km radius of the surface center. Figures 4a – 4c show a time evolution of the vertical profiles of relative humidity, averaged over the various ensemble members grouped by final intensity (WEAK, AVERAGE, STRONG), while Figs. 4d – 4f show the vertical profiles for the eight weakest ("8WEAKEST") and eight strongest

("8STRONGEST") ensemble members according to final intensity, as well as the respective group means. Throughout nearly the entire depth of the troposphere, the ensemble members that fail to develop have relative humidities that are on average less than those of the ensemble members that do intensify. This difference between intensity groups is especially apparent in the mid-levels (between 4 and 7 km). As early as 12 hours into the simulation, the mean vertical profile of the weakest members (WEAK) is about 10% drier at the low- and upper-levels when compared with the STRONG vertical profile. At mid-levels, this difference is as large as 20%. As the simulation progresses, the difference between the mean profiles at the low- and upper-levels remains around 10%, however, the difference at the mid-levels increases to around 25%. The difference between the composite profiles 8WEAKEST and 8STRONGEST members at this time is as large as 30%.

Similarly, a time evolution of vertical profiles of 200-km area-averaged equivalent potential temperature (K) averaged according to final intensity is constructed (Figs. 5a–c). Once again, throughout the complete vertical profile, the equivalent potential temperatures for the WEAK members are on average less than the STRONG members. Because the mid-level temperature profiles of the ensemble members are very similar (not shown), these lower equivalent potential temperatures correspond to drier air, and therefore lower mixing ratios associated with the weaker members. Figures 5d–f show the equivalent potential temperature vertical profiles of 8WEAKEST and 8STRONGEST. The difference between these intensity groups is once again evident throughout the profile, but is most noticeable between 4 and 7 km, which is the same level where the greatest difference in relative humidity can be seen. The evolution of the structure of these profiles suggests that many of the weaker members may fail to intensify due in part to intrusions of dry air at mid-levels.

The top two rows of Fig. 6 show a time evolution of storm-centered composite 500-hPa relative humidity (%) for 8WEAKEST and 8STRONGEST, respectively, while the bottom row shows the difference between the two groups. It should be noted that the ensemble members of 8WEAKEST have the highest minimum SLPs at forecast hour 42 but are not necessarily the 8 weakest ensemble members at each of the times of the composites. These composites display data for a 600-km by 600-km box around the surface center of each member and composite geopotential height contours at 500-hPa are also overlaid. Both sets of relative humidity composites exhibit similar structures. Moister air is located predominantly to the southeast of the storm centers with drier air to the west and northwest of the storm centers. The areas of higher relative humidity are associated with the areas of the strongest convection. Differences between the composites arise however, as the region of very moist air covers a much larger area in the 8STRONGEST composites. This moist air is not only located to the southeast of the storm centers, but also to the east and northeast of the centers. In these regions, the relative humidities in the 8STRONGEST composites are as much as 40% higher than in the 8WEAKEST composites (Figs. 6g – 6i). The composites also indicate not only moister air (at least a 10% – 20% difference throughout the cross-section) for the stronger members, but this moister air is located over the surface circulation centers of the members. It appears that the drier air located over the surface circulation centers of the 8WEAKEST members may be preventing the weaker members from developing. These spatial composites provide strong indications of dry air intrusions into the centers of the weak ensemble members at 500-hPa. Figure 6 also clearly illustrates the difference in mid-level vortex strength between the groups by comparing the geopotential height contours of the composites. By 1200 UTC 2 September, the 8STRONGEST composite has a closed and much stronger composite vortex that deepens throughout the

simulation. The composite vortex of the 8WEAKEST members is much weaker, and a closed vortex cannot even be identified.

The evolution of the structure of the composites for the two intensity groups at 700-hPa (not shown) is similar to the composites at 500-hPa, with moist air to the east of the surface circulation centers and drier air to the west. Even more influential at this level than at 500-hPa, the moister air envelops the circulation center of the stronger member composite, while lower relative humidity air (typically about 70% for 8WEAKEST compared to 80% for 8STRONGEST) is located over the circulation center of the weaker members. It is also worth noting that in the 8STRONGEST composites at both 500-hPa (Figs. 6d – 6f) and 700-hPa (not shown), as early as twelve hours into the simulation, there is an area of drier air that appears to be slowly wrapping around the outside of the center of circulation. This feature may result from the stronger initial intensities of the stronger ensemble members. More intense vortices associated with the strong members can more rapidly advect the surrounding dry air around the center of the storms. This helps prevent the dry air from being advected into the circulation center by the surrounding environmental flow and makes dry air intrusions in the stronger members less likely. This suggests that there may be a more complex relationship between atmospheric moisture and tropical cyclone intensity that will be further investigated later.

Figure 7a and 7c show a time evolution of the composite vertical profiles of relative humidity for 8WEAKEST and 8STRONGEST, respectively. These plots effectively synthesize the information displayed in Fig. 4 and further highlight the differences between the composite groups. Similar results are seen when plotting the composite vertical profiles of relative humidity for the WEAK, AVERAGE and STRONG groups (not shown), although the differences in magnitude are not as large. It is once again clear from these figures that the weak members tend

to have a consistently drier vertical profile at all times. The difference between the composites is the clearest at the mid-levels as the members of the 8STRONGEST group have moister air (relative humidities between 70% and 80%) while the members of the 8WEAKEST group develop drier air (relative humidities between 50% and 70%) in this region, particularly as the simulation evolves. Similar composite vertical equivalent potential temperature profiles (θ_e, not shown) illustrate that the θ_e values are lower for the weaker ensemble members, almost exclusively in the mid-level region between 4 and 8 km. These results are once again consistent with the observations concerning the composite vertical profiles of relative humidity.

Figure 7b shows the time evolution of the correlation at each height and time between the 200-km area-averaged relative humidity (%) and the final intensity in terms of minimum SLP of the 60 ensemble members. Therefore, a negative correlation implies that there is moister air (higher relative humidity) when the storms are more intense (lower minimum SLP). As expected, the relationship between the relative humidity and final intensity is strongest in the mid-levels. Twelve hours into the simulation, the correlation between relative humidity in the 4 to 7 km region and final intensity is moderate (approximately -0.55). By forecast hour 24, which is the point in the simulation where the intensities of the ensemble members really begin to separate, the correlation has become strong (approximately -0.70). These calculations provide statistical evidence of the importance of the mid-level moisture in determining the final intensity of each ensemble member. These results are consistent with the physical expectation that the atmospheric moisture profile will influence intensity.

Figure 7d shows the time evolution of the partial correlation between the 200-km area-averaged relative humidity and the final intensity, with the current intensity held constant. This calculation is performed to remove the effect that the current intensity of each member has on the

statistical relationships. The partial correlation will steadily decrease over time regardless, and will reach zero by forecast hour 42 when the final intensity is equal to the current intensity. Overall, as expected, the partial correlation is weaker than the correlation, as the current intensity in general has some impact on the final intensity. However, at forecast hour 12, a moderate correlation (approximately -0.55) still exists between the relative humidity and the final intensity at the mid-levels. This correlation remains weak to moderate in the simulation until forecast hour 27, which is the point when the current intensity has a larger impact on the final intensity spread. These results provide more evidence of the importance of the mid-level moisture between forecast hour 12 and 24 in determining the final intensity of each member in the ensemble.

To more clearly illustrate the impact of the mid-level dry air intrusions, correlation contour plots are constructed of horizontal cross-sections of relative humidity. Figures 8a – 8c show a time evolution of the storm-centered ensemble mean 500-hPa relative humidity (%) field, while Figs. 8d – 8f show these same plots at the 700-hPa level. The overall structures of the ensemble mean relative humidity fields are as expected very similar to the 8WEAKEST and 8STRONGEST composites, with moister air to the east of the surface circulation center and drier air to the west. The ensemble mean wind field at the respective pressure level is also overlaid and throughout the simulation it is clear that the mean circulation centers at 500-hPa and 700-hPa are displaced from the surface center. This indicates that there is a definite tilt of the center with height in the majority of the ensemble member vortices, which is a typical feature of weak and/or sheared tropical storms (Reasor et al. 2004).

Correlation contours between each grid point of the horizontal cross-section of relative humidity and final intensity are also plotted in Fig. 8. The regions with the strongest horizontal gradient in relative humidity are those with the highest correlation. Due to the negative

correlation, the ensemble members with stronger final intensities (lower minimum SLPs) will have higher relative humidities in these regions. At the 500-hPa level at forecast hour 24, the region of significant correlation encompasses a fairly large area surrounding the surface circulation. This result does not necessarily indicate the individual dry air intrusions at this level, but it does show that the stronger ensemble members on average have uniformly higher relative humidities across the tropical storms. The correlation analysis at the 700-hPa level provides more evidence of dry air intrusions. At forecast hour 24, the area of moderate correlation that appears to have originated northwest of the mean surface circulation, over the driest region, has extended southeast towards the centers of the members across the region of the largest gradient. Once again this implies that the most significant difference between the moisture fields of the weak and strong ensemble members occurs in this region. This correlation structure is consistent with dry air northwest of the center being advected into the circulation center, preventing the weaker ensemble members from intensifying. The correlation contours indicate that these dry air intrusions do not occur as often or as detrimentally for the ensemble members that intensify.

Vorticity

Besides the mid-level atmospheric moisture, another important factor in the intensity determination of a member is the initial and subsequent evolution of the vorticity of the member. Sippel et al. (2011) found that initial low-level potential vorticity was the factor most strongly correlated with final intensity of Tropical Storm Debby (2006). Figures 9a - 9c show a time evolution of the 200-km area-averaged relative vertical vorticity (10^{-5} s^{-1}) profiles averaged according to final intensity. At forecast hour 12 it is clear that the members of STRONG have initially higher relative vorticities throughout the entire vertical profile. A stronger initial vortex not surprisingly seems to lead to a stronger final vortex as a relationship exists between the

current intensity and final intensity of the storm. As the storms evolve, the stronger members maintain higher relative vorticities at all heights, which correspond with stronger circulations. Figures 9d - 9f show a time evolution of the 200-km area-averaged relative vorticity (10^{-5} s^{-1}) profiles for the 8WEAKEST and 8STRONGEST ensemble member groups. The profiles of these extreme performing members once again demonstrate the differences in vorticity between the members of the two intensity groups. Increases in the vorticity in the mid-levels of the vertical profiles for the members in 8STRONGEST are observed as the simulation evolves. The vorticity profiles of the members in 8WEAKEST however, remain mostly unchanged.

Once again, statistical correlations are used to determine if the differences in the relative vorticity profiles between the intensity groups are statistically significant. Figures 10a and 10c show a time evolution of the 200-km area-averaged relative vorticity composites of 8WEAKEST and 8STRONGEST. These plots continue to highlight the increase in relative vorticity for the stronger members as the simulation evolves. The vortices associated with the 8STRONGEST members appear to be intensifying throughout most of the vertical profile but particularly in the mid troposphere, throughout the simulation. Figure 10b shows a time evolution of the correlation between the 200-km area-averaged relative vorticity profile and the final intensity of each ensemble member. As early as forecast hour 12, the correlation between relative vorticity and final intensity is moderate throughout the profile. By forecast hour 15, the correlation has increased and is particularly strong in the mid-levels (between 3 and 8 km). The correlation between the relative vorticity and final intensity is stronger and appears to increase earlier in the simulation than the correlation between the relative humidity profiles and the final intensity. This implies that the current relative vorticity could prove to be a very useful factor in determining whether an ensemble member intensifies or not.

Figure 10d shows a time evolution of this partial correlation between the 200-km area-averaged relative vorticity profiles and the final intensity with the current intensity held constant. The partial correlation is significantly weaker than the correlation but as early as forecast hour 15 a moderate partial correlation is seen in the mid-level region of the relative vorticity profile, corresponding to stronger and deeper vortices in the stronger ensemble members. This moderate partial correlation is an indication that although relative vorticity is sometimes considered to be a measure of the intensity of a tropical cyclone, in this simulation the two are not interchangeable. An increase in relative vorticity in the developing members of this simulation is observed before a corresponding drop in minimum SLP and this provides an indication that relative vorticity may offer a signal that a given ensemble member is about to strengthen. The relative vorticity partial correlation profile is similar to the partial correlation results from the relative humidity and the θ_e analysis, indicating that both the atmospheric moisture and vorticity play a role in determining the final intensity of the ensemble members in this simulation.

The relationship between relative vorticity and convection is also investigated in order to potentially add another factor that can be utilized in predicting the final intensity of a given ensemble member. Figure 11 shows a time evolution of the composite 2-km radar reflectivity (dBZ) fields for the 8WEAKEST (Figs. 11a – 11c) and 8STRONGEST (Figs. 11d – 11f) ensemble groups. These composites demonstrate that the ensemble members with the stronger final intensities, and therefore the stronger initial vortices, have a larger areal coverage of convection as well as more intense convection associated with the storms. It appears that the members of 8STRONGEST also develop convection located closer to the circulation center than the members of 8WEAKEST, even though the convection in both intensity groups is located almost exclusively to the east of the surface circulation center. The presence of convection in

these ensemble members must also influence the atmospheric moisture profiles of each of the members, highlighting the complicated interactions that exist in this simulation between both thermodynamic and dynamic variables. Given the randomness of moist convection, these interactions may further limit the predictability of Erika's evolution and final intensity.

Relationship between Thermodynamic and Dynamic Processes

The results of the correlation analysis of the atmospheric moisture variables and the intensity variables revealed that both thermodynamic and dynamic processes are important in determining the final intensity of an ensemble member in this simulation. The time evolution of the correlation and partial correlation plots from the relative humidity and the relative vorticity analyses have very similar magnitudes and structures, and therefore reveal a potential relationship between the two variables. A simple way to test the relationship between these two variables is to once again use a basic statistical correlation. Figure 12a shows a time evolution of the correlation between the 200-km area-averaged relative humidity (%) and the 200-km area-averaged relative vorticity (10^{-5} s^{-1}). As early as 9 hours into the simulation, a moderate correlation exists between the vorticity and the low- to mid-level (2-5 km) relative humidity field. As the vorticity develops in the low- and mid-levels of the profile as the ensemble members begin to intensify, the correlation also increases at these levels. By forecast hour 21, there is a strong correlation between the vorticity and the relative humidity. By this time in the simulation, the separation in intensity between the strong developing members and the weaker members has begun. This can be clearly illustrated by examining the time evolution of the correlation between current intensity and final intensity in terms of minimum SLP (Fig. 12b). The correlation at forecast hour 21 is approximately 0.60, which is moderate. There is also a correlation between the current and final intensity, which is initially weak (~0.3) and remains

weak to moderate throughout the majority of the simulation period. This relationship is also illustrated by the results of the partial correlation analyses.

The strong correlation between the relative vorticity and the relative humidity reinforces the existence of a relationship between the thermodynamic and dynamic processes in the evolution of Erika. A complicated feedback process between these two variables is occurring, although it is difficult to determine whether the dynamic processes or the thermodynamic processes are more important. The correlation between relative humidity and final intensity and the correlation between relative vorticity and final intensity become significant near the same time in the simulation (forecast hour 12), although the correlation between relative vorticity and final intensity is much stronger. There appear to be two potential scenarios that dictate whether an ensemble member will intensify or not. If the thermodynamic variables are more influential on the intensification process, an analysis of the mid-level relative humidity profiles will reveal dry air intrusions that infringe upon the circulation centers of the eventually weaker ensemble members. These dry air intrusions are detrimental to the development and intensification of convection in the tropical storm. In this situation, the thermodynamic profiles and whether or not a dry air intrusion occurs will be the dominant contributor to whether intensification occurs or not, thereby dictating the dynamics. However, if the dynamic variables are more influential on the intensification process, the stronger initial vorticity and therefore circulation can prevent dry air intrusions from occurring by advecting the drier air around the outer circulation of the storm, inhibiting the dry air from reaching the circulation center. In addition, the storms with stronger initial vortices tend to have a larger areal coverage and intensity of convection associated with them, and outer rainbands can therefore protect the inner core from the dry air intrusions (Kimball 2006). This process would allow the tropical system to maintain a moist profile over

the center of the vortex and intensification could proceed. In this scenario, the stronger initial vorticity, which is a dynamic variable, is more significant in the determination of intensification. Regardless of which group of variables is more important, the correlation analysis of these factors reveals that a complex relationship exists between the thermodynamic and dynamic variables in this simulation, emphasizing the importance of both of these groups of variables.

Deep Layer Shear

The final environmental factor considered that has an influence on the final intensity spread in this study is the deep-layer (850 hPa – 200 hPa) wind shear. We focus on this environmental factor primarily due to the well-documented negative effects of deep-layer shear on tropical cyclone intensification (Simpson and Riehl 1958; Gray 1968; DeMaria and Kaplan 1994, 1999; and others) as well as the frequent appearance as an important factor in similar predictability studies (Sippel and Zhang 2008). Figure 13a shows the ensemble mean deep-layer shear magnitude and direction for this simulation. The magnitudes of shear for each ensemble member are calculated by taking the average of the difference in wind velocities between the 850-hPa and 200-hPa level at every model grid point that is between 200-km and 500-km from the surface center. The values are then averaged across the members and plotted in Fig. 13a. The observational data discussed in the introduction (AMSU data) as well as the Statistical Hurricane Intensity Prediction Scheme (SHIPS; DeMaria et al. 2005) shear are also overlaid in Fig. 13a. Throughout the simulation, the magnitude of the ensemble mean shear remains moderate, in the range of 10 – 15 kts. The mean southwesterly shear present during the first day of the simulation begins to evolve towards a westerly shear around forecast hour 24 (approximately 240° – 280°). The observational estimates of the magnitude and direction of the deep-layer shear are similar to the results from the ensemble simulation. The initial magnitude of the AMSU shear (30 kts)

appears to be larger than in the simulations, but throughout the rest of the lifetime of Tropical Storm Erika the observed shear remains between 10 and 20 kts, which is fairly consistent with the simulation. The direction of the observed AMSU shear is also fairly similar to the simulated shear, although the observed shear is predominantly southwesterly throughout the entire simulation (approximately 240°) and does not becomes more westerly with time. The magnitude and direction of the SHIPS shear is even more comparable to the ensemble mean shear. The similarities between the observed and simulated shear provide confidence that the thermodynamic and dynamic processes occurring in the ensemble simulation could be representative of those within Tropical Storm Erika.

Based on the results shown in Fig. 13a, the ensemble mean direction of the deep-layer shear and the location of the convection in the ensemble members appear to be related. Figure 11 shows a time evolution of the composite 2-km radar reflectivity (dBZ) for 8WEAKEST and 8STRONGEST. In addition to the reflectivity, mean deep-layer shear vectors are plotted from the composite centers and are pointed in the direction of the shear. It is clear from these plots that simply being in the presence of this moderate southwesterly shear has displaced all of the convection in the composites eastward of the circulation centers, or downshear. These results are consistent with numerous previous studies, including (for example) the numerical study by Rogers et al. (2003) and the observational study by Corbosiero and Molinari (2002), which found that in the presence of moderate shear, there is a strong preference for convection to be located downshear, both near the storm core and in the outer band region. At forecast hour 12 (Figs. 11a and 11d) and forecast hour 18 (Figs. 11b and 11e) of the simulation, the shear vectors in both the 8WEAKEST and 8STRONGEST composites are of similar moderate magnitude. However, at forecast hour 24, the composite shear vector associated with the weak members has increased

and is now larger in magnitude than the shear associated with the strong members (~11 kts for 8WEAKEST and ~6 kts for 8STRONGEST).

The composite magnitude of center tilt with height of the ensemble vortices is also plotted in Fig. 11. The center tilt with height of each ensemble vortex is calculated by finding the horizontal difference between the 850-hPa center and the 500-hPa center. At forecast hour 12 and forecast hour 18 the center tilt with height of the 8WEAKEST composites and the 8STRONGEST composites are similar and relatively large. At forecast hour 24 the magnitude of the composite tilt vector for 8STRONGEST has become small while the 8WEAKEST composite tilt remains large. An increase in shear over the 8WEAKEST composite and a decrease in center tilt with height over the 8STRONGEST composite at this time also corresponds with the beginning of the intensification period for the strong members. It appears that the relatively weak shear and subsequent reduction in center tilt with height contributes to the intensification of the 8STRONGEST members, while the comparatively stronger magnitude of the deep-layer shear over the 8WEAKEST composite may be preventing intensification from occurring.

It has been shown that the magnitude of the tilt of the vortex increases with increasing shear (Davis et al. 2008) and how the vortex responds to the shear plays a significant role in whether development occurs or not. In addition, in this case, the shear may be preventing the convection from becoming located near the circulation center and the increase in magnitude of the shear of the 8WEAKEST group may be preventing the convection from wrapping around the vortices, which makes intensification difficult. It is important to remember however, that the initial strength of the convection associated with the 8STRONGEST group is stronger and also must be considered as a potential factor that may contribute to the significant final intensity spread. While the shear and tilt vectors in the composites in Fig. 11 indicate that a difference in

shear magnitude may contribute to whether an ensemble member intensifies or not, a more quantitative approach must be used to determine whether this potential relationship exists or not.

Figure 13b shows the time evolution of the area-averaged deep-layer (850 hPa – 200 hPa) shear averaged according to final intensity. Between forecast hour 12 and 15 the deep-layer shear of the ensemble members that eventually intensify (STRONG) continues to decrease in magnitude, while the shear associated with the weak ensemble members (WEAK) persists. Although throughout the rest of the simulation an observable difference in shear can be seen, the difference in magnitude between the two intensity groups is only a few knots (approximately 11 kts of shear over the WEAK group and approximately 7 kts of shear over the STRONG group). Figure 13c shows a time evolution of the correlation between area-averaged deep-layer shear and final intensity for this simulation of Tropical Storm Erika. Between forecast hour 12 and 15 the correlation does begin to increase, corresponding with the same time when the magnitudes of the wind shear for the intensity groups begin to diverge. The correlation peaks at approximately forecast hour 24, coincident with the time of intensity divergence, but only at a weak value of just over 0.3. For the rest of the simulation, the correlation decreases and is nearly zero by the end of the simulation. Figure 13d shows a scatterplot of final intensity versus area-averaged deep-layer wind shear at forecast hours 12, 18, and 24 for the ensemble members that compose 8WEAKEST and 8STRONGEST. There is an indication, particularly at forecast hour 24, that the members of 8STRONGEST always have values of deep-layer shear that are weak, while the 8WEAKEST members have a much wider spread of shear values. Therefore, there is evidence that the stronger values of shear may prevent intensification from occurring in some of the weaker ensemble members, however, a lack of shear does not guarantee intensification. A relationship between deep-layer shear and final intensity exists, but the results of this correlation

analysis are not as strong as the results from the correlation analyses of atmospheric moisture and absolute vorticity.

Even though the correlation between deep-layer shear and final intensity is not as significant as are the correlations between intensity and some of the other factors, based on the location of the convection associated with the ensemble members it is clear that the deep-layer shear has an impact on the evolution of this simulation. Simply the presence of this moderate shear can have a large impact on the atmospheric moisture profiles of the ensemble members, which has been shown to have a statistical impact on final intensity, by advecting dry air into the circulation centers and thereby preventing intensification. Zhang and Tao (2012) have also shown that even in the presence of weak to moderate vertical wind shear, particularly during the development stage, nearly identical initial conditions among ensemble members can produce a very significant intensity spread. They also showed that the forecast uncertainty increased with increasing strength of the shear. Although the simulated storms in the Zhang and Tao (2012) study are initially much weaker than this ensemble simulation of Tropical Storm Erika, this phenomenon may be occurring in this simulation, with the vertical wind shear significantly influencing the other factors such as atmospheric moisture and vorticity, which in turn creates a significant spread in intensity. The presence of weak to moderate vertical wind shear associated with the ensemble members in this simulation limits the predictability of the intensity of Erika.

CHAPTER 4: Conclusions

A 60-member ensemble WRF simulation of Tropical Storm Erika was performed and analyzed to assess the predictability of this weak tropical storm that was forecast by operational models to intensify into a hurricane but failed to actually do so. The predictability of this poorly forecasted system has been found to be quite limited given realistic initial and boundary conditions from the real-time GFS-EnKF. The factors that contribute the most to the significant intensity spread have been determined through a correlation analysis. In addition, the use of partial correlations has allowed for a more robust analysis of the inherent relationships that exist between the various factors. These factors are found to be the mid-level atmospheric moisture profile, the absolute vorticity and the deep-layer wind shear. Dry air intrusions into the circulation centers of the weak ensemble members between the 500-hPa and 700-hPa levels appear to prevent these members from intensifying. Determining the cause of the dry air intrusions is slightly more complicated. It appears that these intrusions are caused by a combination of ambient environmental dry air and the advection of this dry air into the centers by moderate deep-layer wind shear. In some of the stronger ensemble members with stronger initial vortices, these dry air intrusions are prevented by the advection of dry air away from the circulation center, due to strong rotational flow. This combination of thermodynamic and dynamic processes prevents some ensemble members from intensifying while allowing others to intensify. Identifying which ensemble members will actually experience dry air intrusions is not straightforward and there is an inherent randomness involved with these processes. However, a weaker initial intensity or an increase in magnitude of deep-layer wind shear raises the probability of a dry air intrusion occurring and intensification failing to occur.

Future work could include further analyzing the ensemble to determine which members are actually experiencing dry air intrusions that are hindering their development. Once the dry air intrusions are more clearly identified, the origins of this dry air can be better assessed and a more concrete determination of which process is causing these intrusions can be made. It should be noted however, that simply the presence of weak to moderate vertical wind shear associated with the ensemble members of this simulation may limit the predictability of this tropical system.

APPENDIX A: Figures

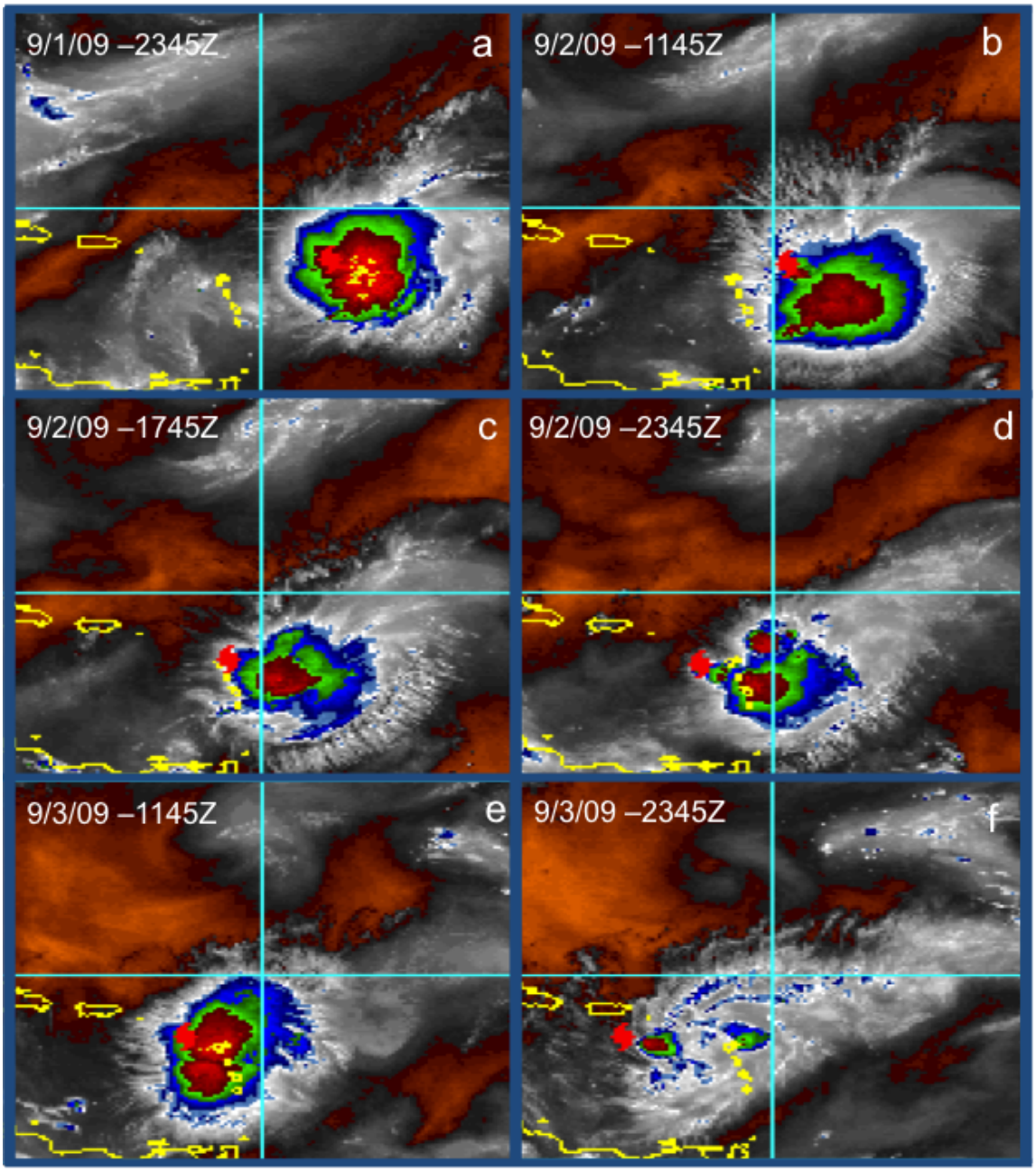

Figure 1. Water vapor satellite images of Tropical Storm Erika from a NOAA satellite at (a) 2345 UTC 1 September 2009, (b) 1145 UTC 2 September 2009, (c) 1745 UTC 2 September 2009, (d) 2345 UTC 2 September 2009, (e) 1145 UTC 3 September 2009, and (f) 2345 UTC 3 September 2009. The center of circulation at each time is indicated by the red hurricane symbol. Burnt orange regions indicate areas of drier air. 20°N and 60°W are also drawn in aqua for reference. Images obtained from: *http://rammb.cira.colostate.edu/products/tc_realtime/storm.asp?storm_identifier=AL062009*.

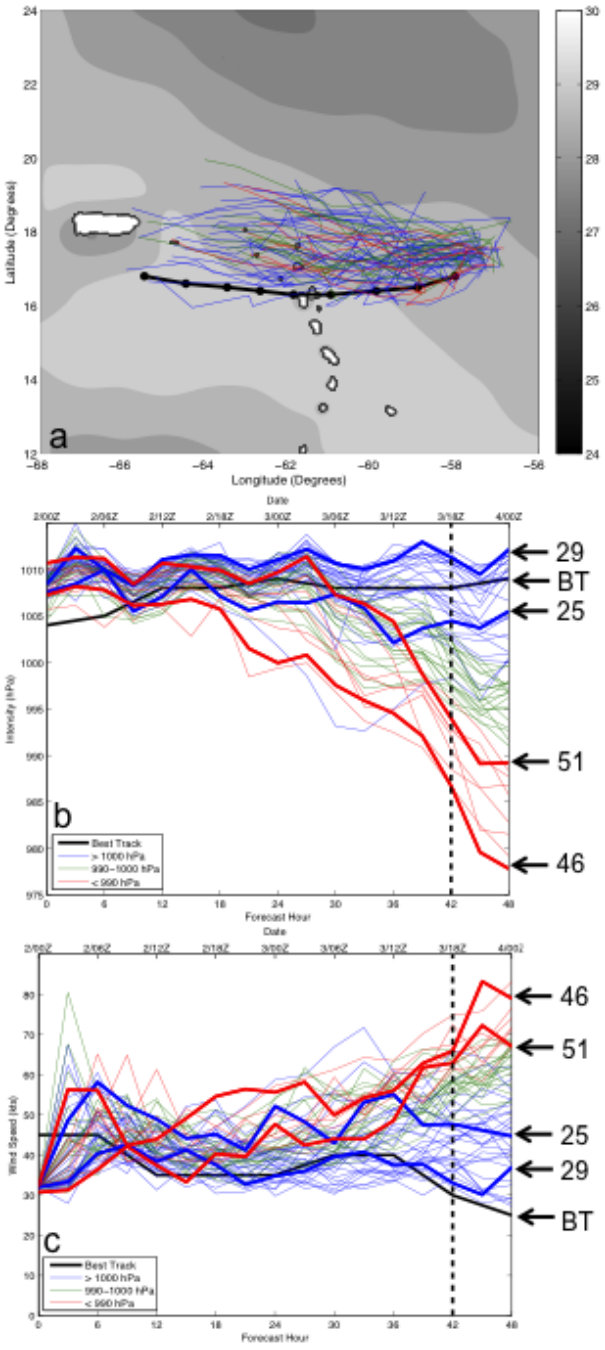

Figure 2. Time evolution of the tracks (a), the minimum SLP in hPa (b), and the maximum wind speeds in kts (c) of the best track of Tropical Storm Erika (black, position indicated every 6 hours in panel a) and the ensemble members grouped by intensity at 1800 UTC 3 September 2009 (WEAK – minimum SLP > 1000 hPa – blue, AVERAGE – minimum SLP between 990 and 1000 hPa – green, and STRONG – minimum SLP < 990 hPa – red). A portion of the inner domain of the WRF simulation is plotted in panel a along with sea surface temperature contours every 1°C. The thick red and blue lines in panels b and c correspond to four selected ensemble members. Members 29 and 25 are two members of WEAK while Members 46 and 51 are members of STRONG.

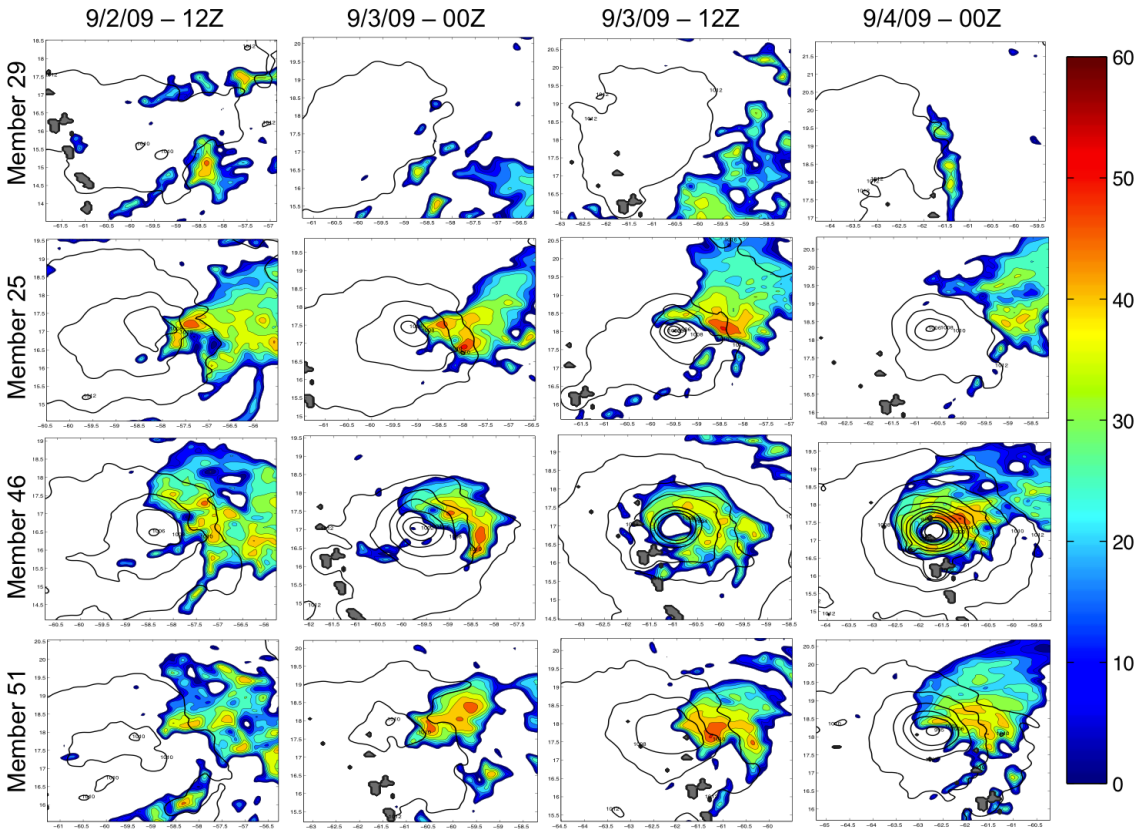

Figure 3. Time evolution (every twelve hours between 1200 UTC 2 September 2009 and 0000 UTC 4 September 2009) of 2-km simulated radar reflectivity (filled contours every 5 dBZ) and sea level pressure (contour lines every 2 hPa between 1000 hPa and 1012 hPa, every 5 hPa for pressures less than 1000 hPa) for the four highlighted ensemble members in Fig. 2. Each panel is storm-centered and the domain encompasses a 5° latitude by 5° longitude box. Radar reflectivity contours have been smoothed (using a 1:2:1 smoother in both the x and y directions) 10 times for clearer visualization.

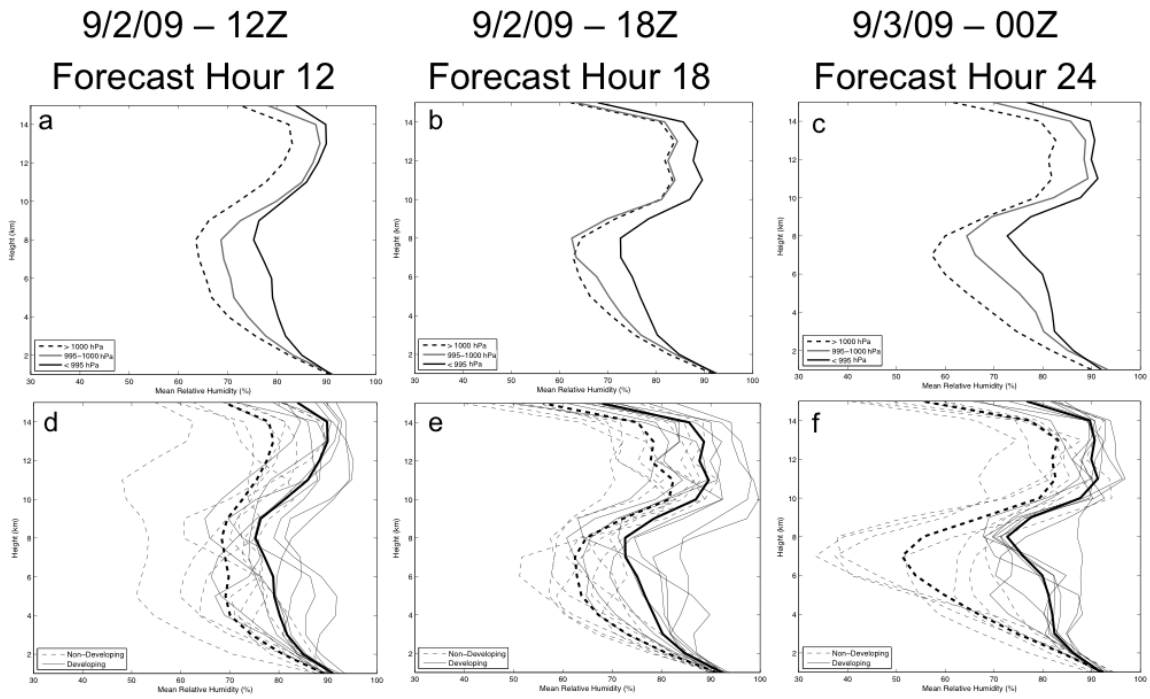

Figure 4. Vertical profiles of 200-km area-averaged relative humidity (%) averaged according to final intensity (WEAK – minimum SLP > 1000 hPa – black dashed, AVERAGE – minimum SLP between 990 and 1000 hPa – gray and STRONG – minimum SLP < 990 hPa – black solid) at (a) 1200 UTC 2 September 2009, (b) 1800 UTC 2 September 2009, and (c) 0000 UTC 3 September 2009. Relative humidities at each vertical level for each ensemble member are calculated by finding the average relative humidity within a 200-km radius from the surface center. Also shown are vertical profiles of 200-km area-averaged relative humidity (%) for the 8 strongest members (8STRONGEST – black solid) and the 8 weakest members (8WEAKEST – black dashed) at (d) 1200 UTC 2 September 2009, (e) 1800 UTC 2 September 2009, and (f) 0000 UTC 3 September 2009. The thick black solid and dashed lines in each of these plots represent the means of the 8STRONGEST and 8WEAKEST groups.

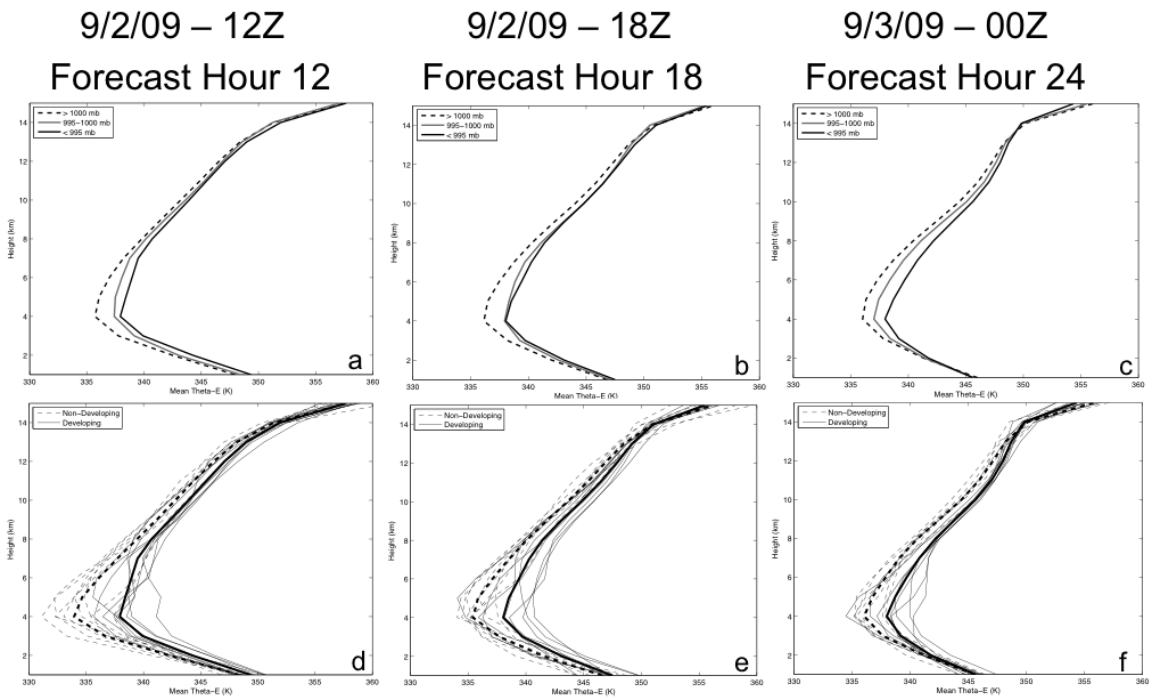

Figure 5. As in Fig. 4 but for equivalent potential temperature (K).

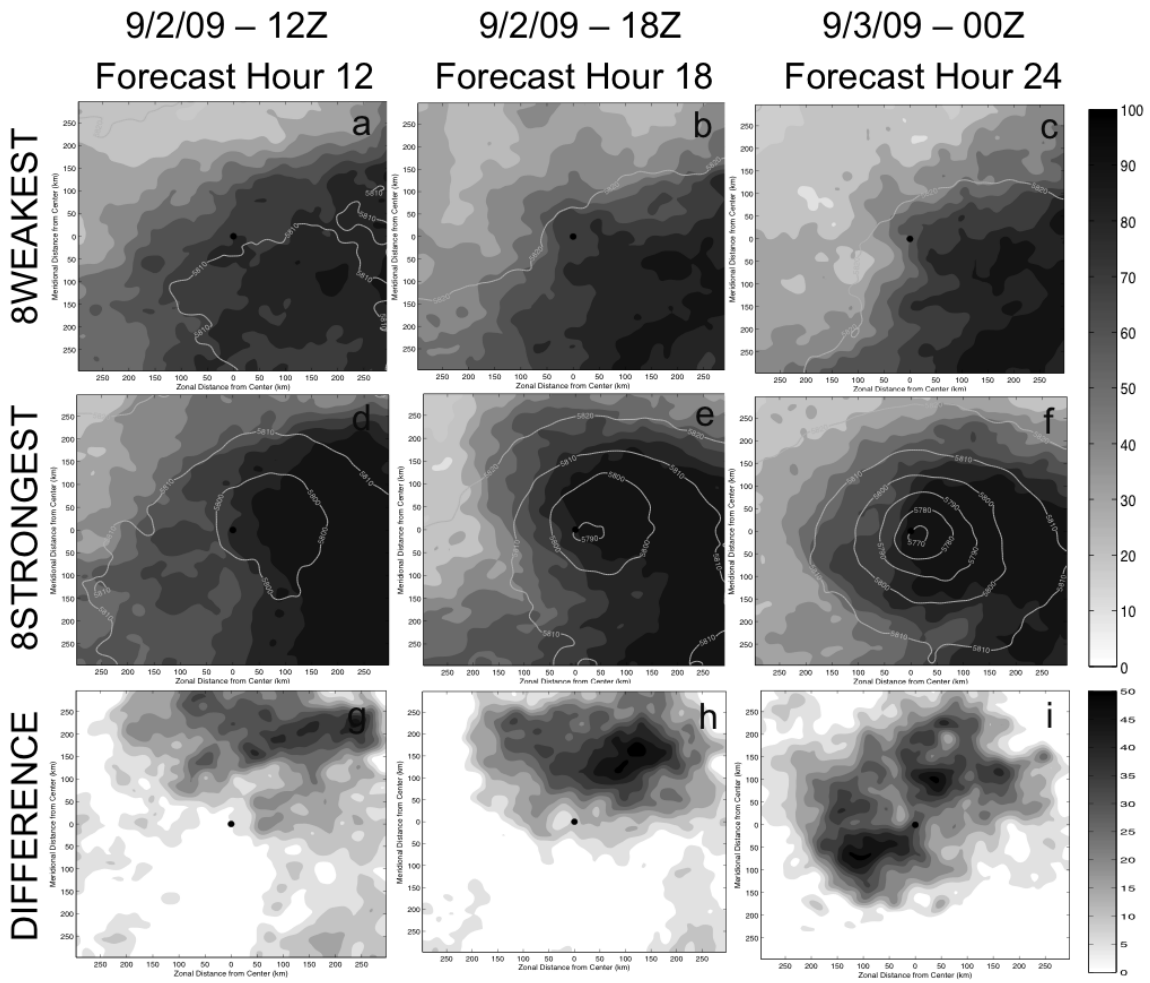

Figure 6. 500-hPa storm-centered horizontal cross-section composites (600-km by 600-km box around each ensemble surface center) of relative humidity (%) (contours filled every 10%) of the 8WEAKEST and 8STRONGEST ensemble member groups at (a and d) 1200 UTC 2 September 2009, (b and e) 1800 UTC 2 September 2009, and (c and f) 0000 UTC 3 September 2009. Geopotential height contours corresponding to the model level whose mean pressure is closest to 500-hPa are also plotted every 5 meters in solid gray. The surface center is indicated by the solid black dot. Relative humidity and geopotential height contours are smoothed 10 times (using a 1:2:1 smoother in both the x and y directions) to aid in visualization. The difference between the relative humidity composites (8STRONGEST – 8WEAKEST) is also plotted at these times (g – i, contours filled every 10%).

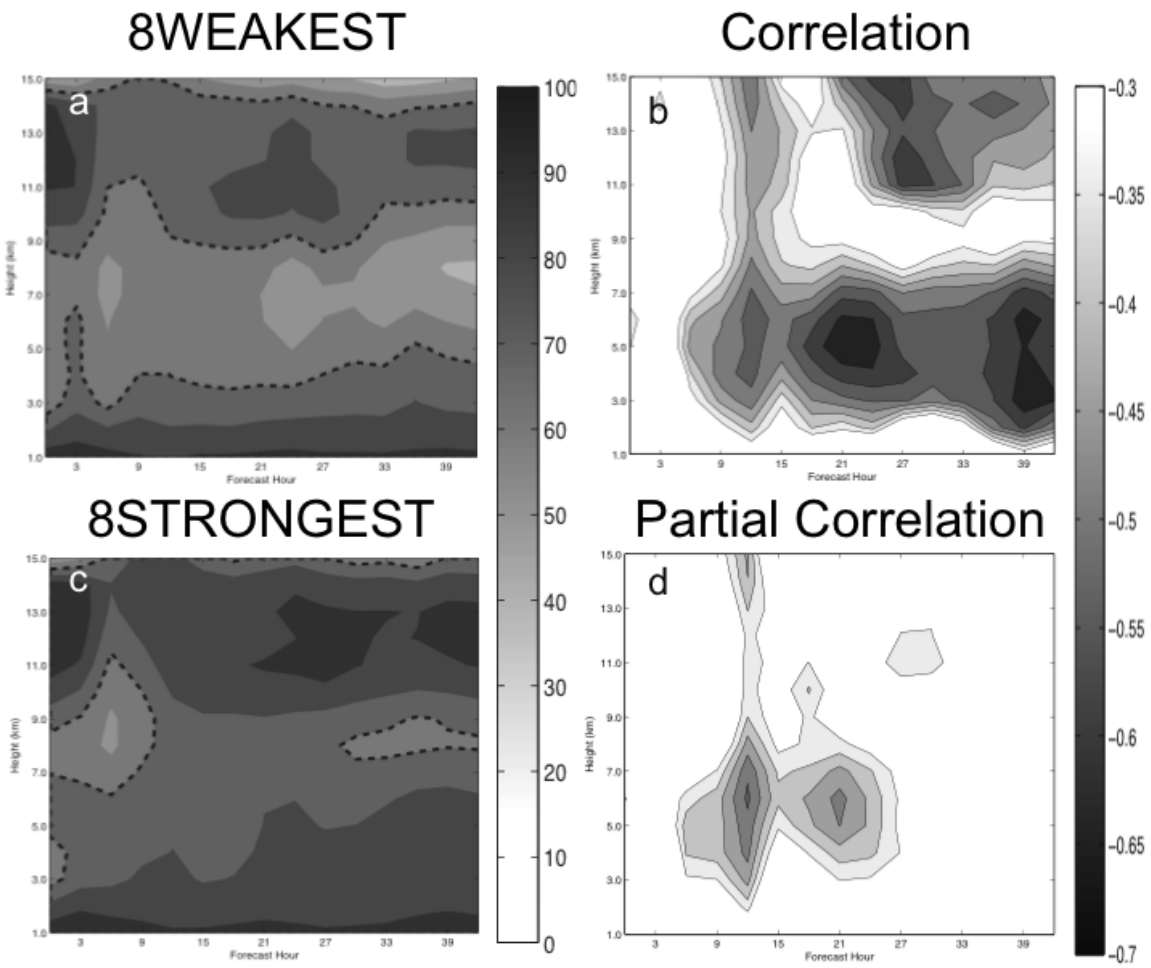

Figure 7. Time-height plots of the composite relative humidity (%) for the 8WEAKEST members (a) and 8STRONGEST members (c). Relative humidity data is plotted every 3 hours and contoured every 10%. The dashed lines indicate the 70% relative humidity contours. (b) Time-height correlation between relative humidity (%) and final minimum sea level pressure at 1800 UTC 3 September 2009. (d) Time-height partial correlation between relative humidity (%) and final intensity with current intensity held constant. Correlation contours are plotted every 0.05 decreasing from -0.3. Since the final intensity is measured by minimum SLP, a negative correlation implies that a higher relative humidity is correlated with a lower (and stronger) minimum SLP.

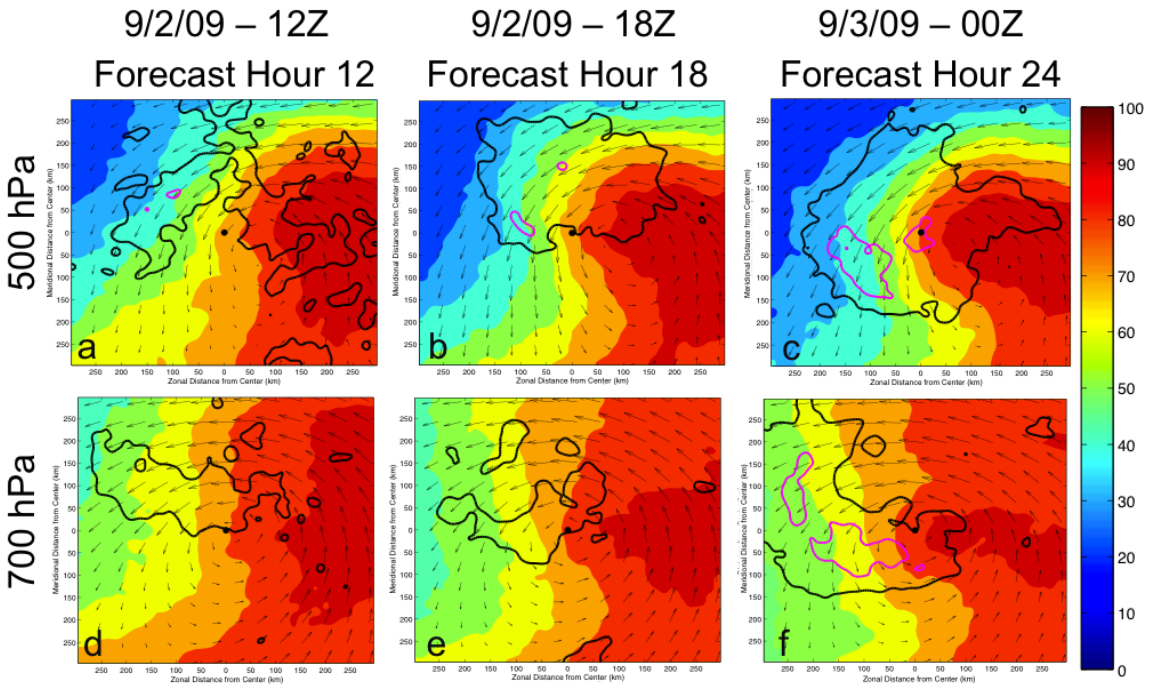

Figure 8. Horizontal cross-sections of storm-centered (surface center) ensemble mean relative humidity at 500-hPa at (a) 1200 UTC 2 September 2009, (b) 1800 UTC 2 September 2009, and (c) 0000 UTC 3 September 2009 as well as at 700 hPa at (d) 1200 UTC 2 September 2009, (e) 1800 UTC 2 September 2009, and (f) 0000 UTC 3 September 2009. Ensemble mean winds at each respective level are also plotted (vectors). Contours of correlation between relative humidity and final intensity are also overlaid (-0.3 in black and -0.5 in magenta). The surface center is also plotted with a black dot. The relative humidity contours (every 10%), ensemble wind vectors and correlation contours are smoothed 10 times (using a 1:2:1 smoother in both the x and y directions) to aid in visualization.

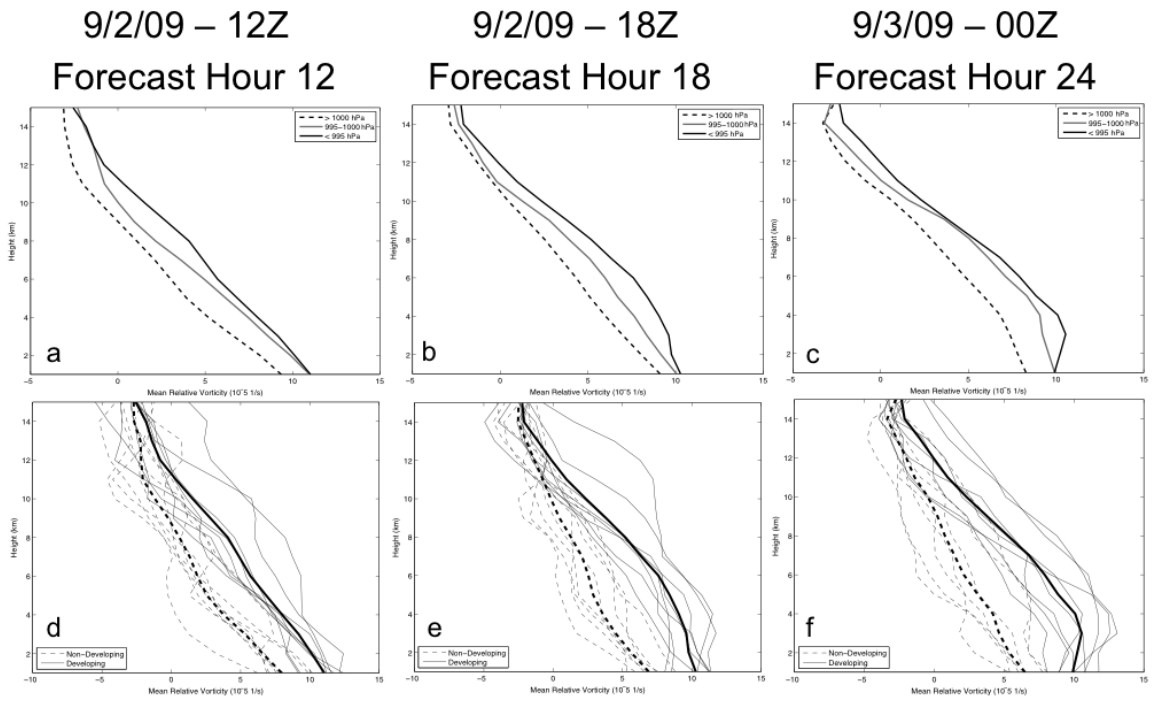

Figure 9. As in Fig. 4 but for relative vorticity (10^{-5} s^{-1}).

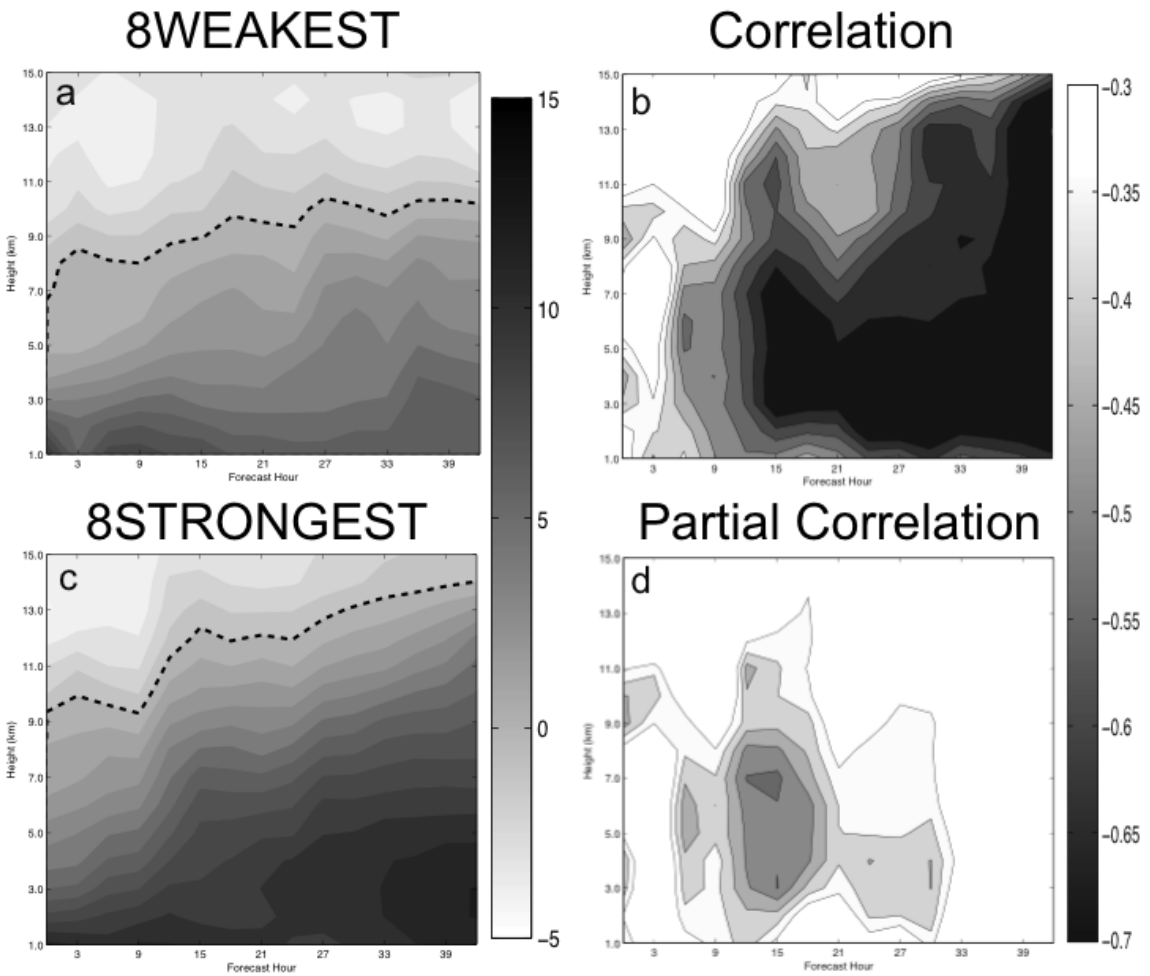

Figure 10. As in Fig. 7 but for relative vorticity (10^{-5} s^{-1}). Relative vorticity is contoured every 10^{-5} s^{-1} and the 0 s^{-1} relative vorticity contour in panels a and c is indicated by a dashed line.

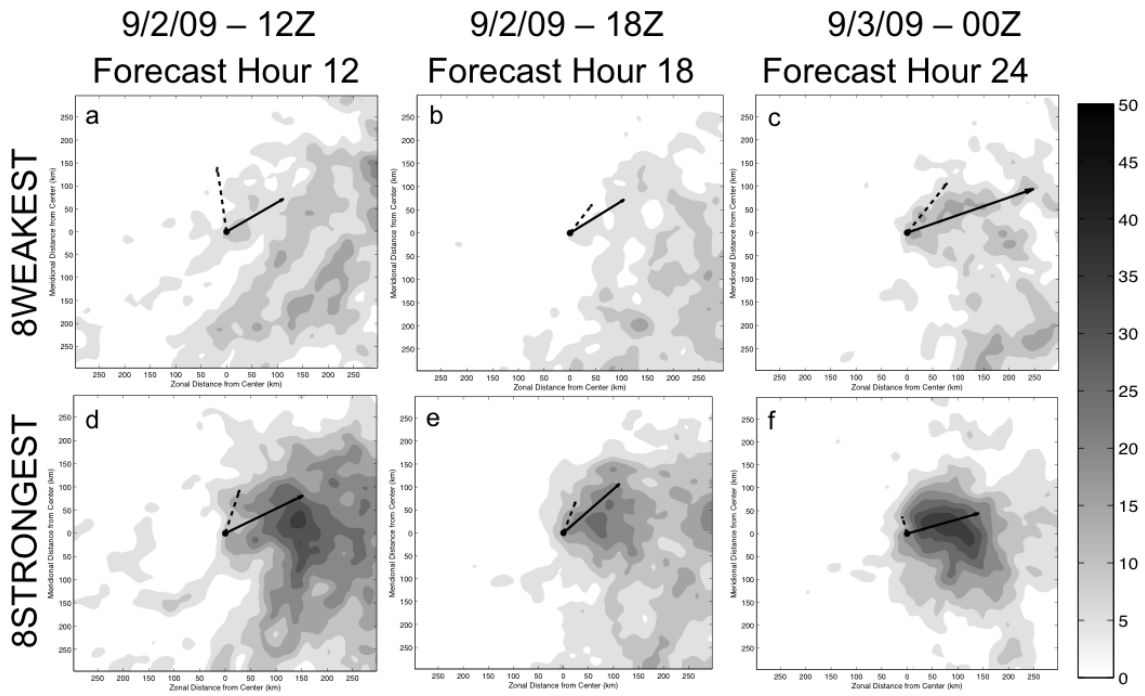

Figure 11. 2-km storm-centered (600-km by 600-km box around each ensemble surface center) simulated radar reflectivity (contoured every 5 dBZ starting at 5 dBZ) composites of the 8WEAKEST and 8STRONGEST ensemble groups at (a and d) 1200 UTC 2 September 2009, (b and e) 1800 UTC 2 September 2009, and (c and f) 0000 UTC 3 September 2009. In addition, composite deep-layer (850 hPa – 200 hPa) shear vectors (calculated by area-averaging shear values between a 200-km and 500-km radius from the center of each member) are plotted in solid black. The direction and magnitude of how the centers tilt with height (between 850 hPa – 500 hPa) is plotted in dashed black. The surface center is indicated by the black dot.

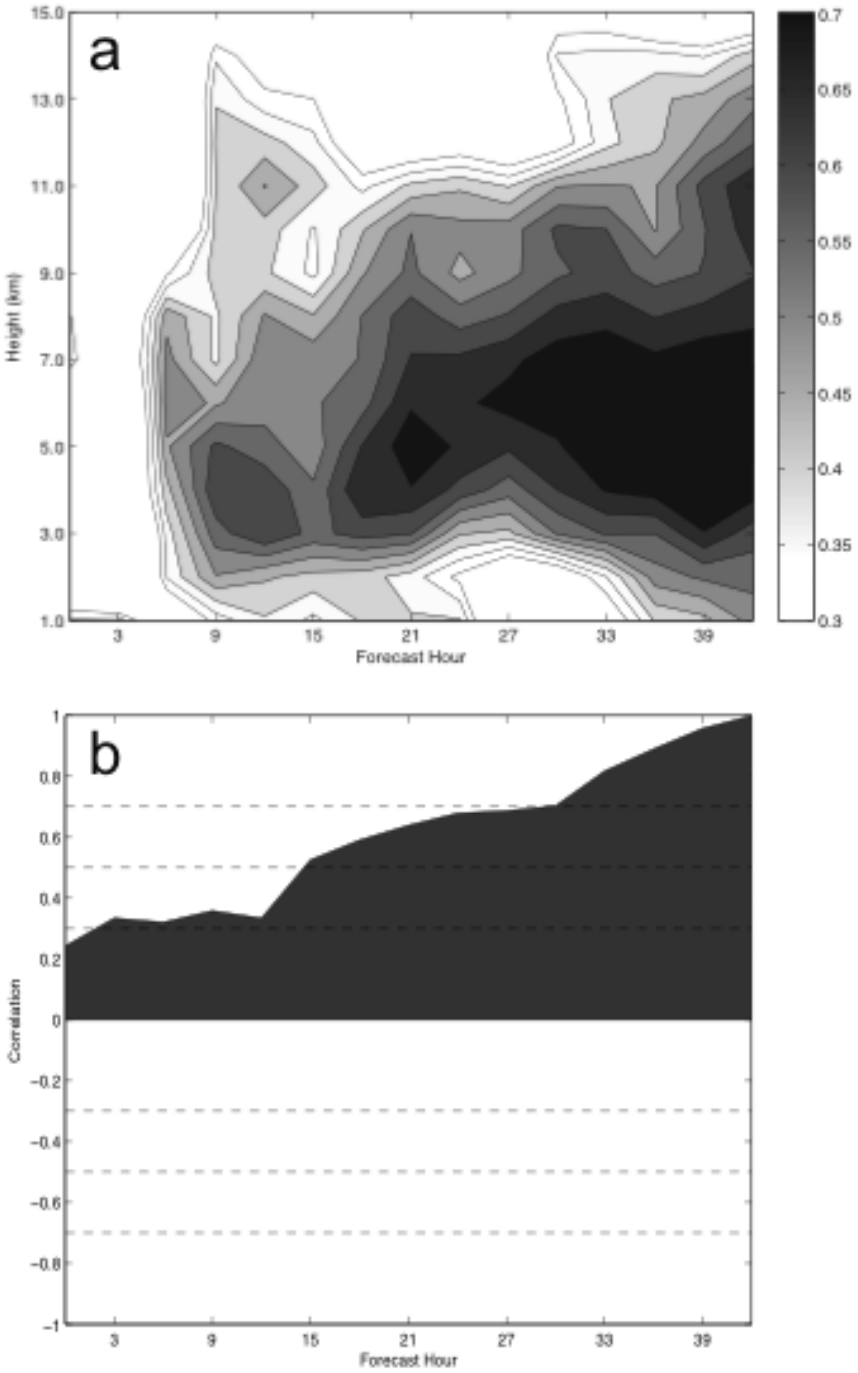

Figure 12. (a) Time-height correlation between relative vorticity (10^{-5} s^{-1}) and relative humidity. Correlation contours are plotted every 0.05 starting from 0.3. (b) Time evolution of the correlation between current minimum SLP and final (at 1800 UTC 3 September 2009) SLP. Correlation equals 1 at forecast hour 42 when the current minimum SLP of each member is identical to the final SLP. The horizontal dashed lines correspond to the defined thresholds of 'weak', 'moderate' and 'strong' (±0.3, ±0.5, and ±0.7) that are used throughout this study.

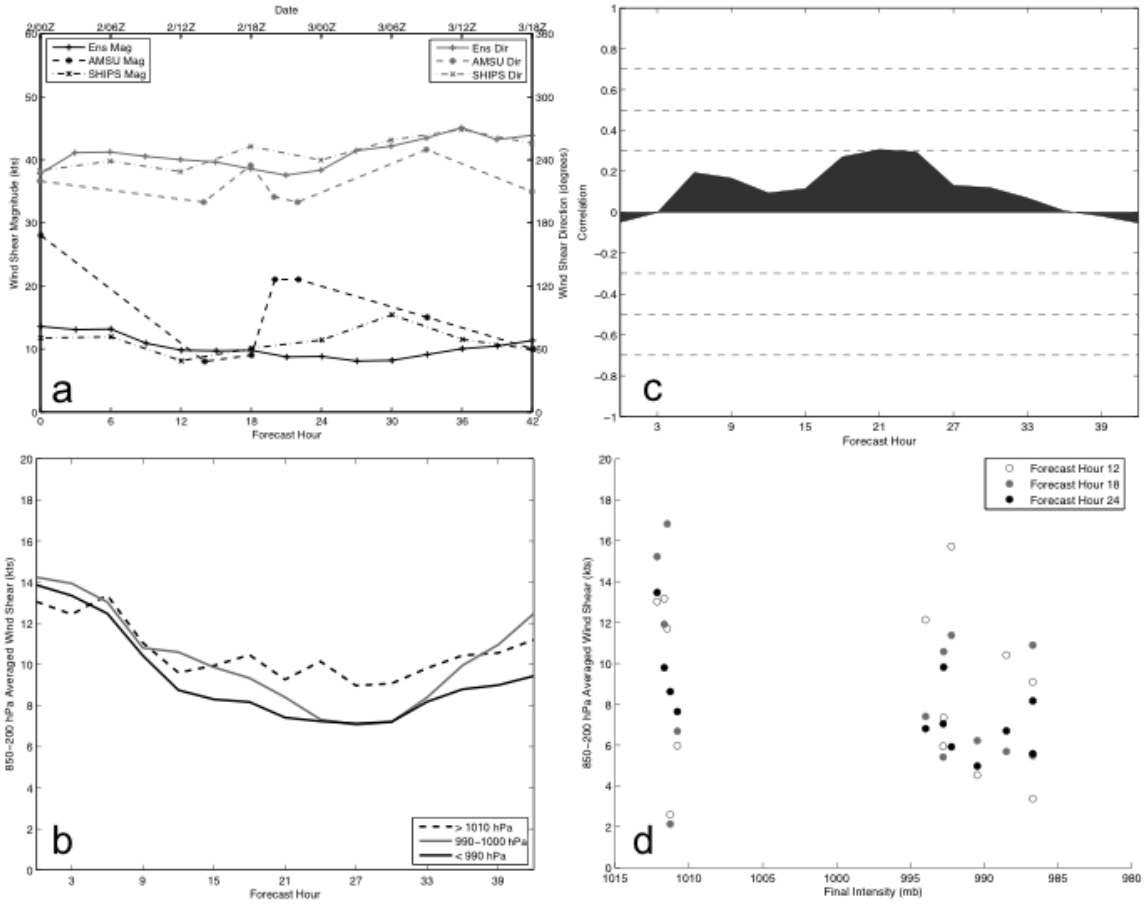

Figure 13. (a) Time evolution of ensemble mean area-averaged deep-layer (850 hPa – 200 hPa) shear magnitude (kts – in solid black) and direction (degrees – in solid gray) for the WRF simulation of Tropical Storm Erika. Also plotted is the time evolution of the AMSU area-averaged deep-layer wind shear magnitude (dashed black) and direction (dashed gray) for a 600-km radius around the center of Tropical Storm Erika and the SHIPS deep-layer shear magnitude (dashed dot black) and direction (dashed dot gray). Observational data obtained from: *http://rammb.cira.colostate.edu/products/tc_realtime/ storm.asp?storm_identifier=AL062009* and *http://rammb.cira.colostate.edu/research/tropical_cyclones/ships/developmental_data.asp*. (b) Time evolution of area-averaged deep-layer (850 hPa – 200 hPa) shear magnitude averaged by final intensity (WEAK – minimum SLP > 1000 hPa – black dashed, AVERAGE – minimum SLP between 990 and 1000 hPa – gray and STRONG – minimum SLP < 990 hPa – black solid). (c) Time evolution of correlation between area-averaged deep-layer (850 hPa – 200 hPa) shear magnitude and final minimum SLP. (d) Scatterplot of final intensity (hPa) vs. area-averaged deep-layer wind shear (kts) at forecast hour 12 (open circles), forecast hour 18 (gray circles) and forecast hour 24 (black circles) for the members of the composite groups 8WEAKEST and 8STRONGEST. Three of the members in the 8WEAKEST group do not have distinguishable circulation centers at forecast hour 42 and therefore are not plotted.

References

Berg, R. J. and L. A. Avila, 2011: Annual summary Atlantic hurricane season of 2009. *Mon. Wea. Rev.,* **139,** 1049 – 1069.

Brown, D. P., 2009: Tropical Storm Erika, 1-3 September 2009. Tropical Cyclone Report. National Oceanic and Atmospheric Administration, National Weather Service, National Hurricane Center, Miami, Florida.

Corbosiero, K. L. and J. Molinari, 2002: The effects of vertical wind shear on the distribution of convection in tropical cyclones. *Mon. Wea. Rev.*, **130**, 2110 – 2123.

Davis, C. A., S. C. Jones and M. Riemer, 2008: Hurricane vortex dynamics during Atlantic extratropical transition. *J. Atmos. Sci.*, **65**, 714 – 736.

DeMaria, M., M. Mainelli, L. K. Shay, J. A. Knaff, and J. Kaplan, 2005: Further improvements to the Statistical Hurricane Intensity Prediction System (SHIPS). *Wea. Forecasting*, **20**, 531 – 543.

DeMaria, M. and J. Kaplan, 1999: An updated Statistical Hurricane Intensity Prediction Scheme (SHIPS) for the Atlantic and eastern North Pacific basins. *Wea. Forecasting,* **14,** 326 – 337.

DeMaria, M. and J. Kaplan, 1994: A Statistical Hurricane Intensity Prediction Scheme (SHIPS) for the Atlantic basin. *Wea. Forecasting,* **9,** 209 –220.

Elsberry, R. L., T. D. B. Lambert, and M. A. Boothe, 2007: Accuracy of Atlantic and eastern North Pacific tropical cyclone intensity forecast guidance. *Wea. Forecasting,* **22,** 747 – 762.

Gray, W. M., 1968: Global view of the origin of tropical disturbances and storms. *Mon. Wea. Rev.,* **96,** 669 – 700.

Hamill, T. M., J. S. Whitaker, M. Fiorino, and S. G. Benjamin, 2011: Global ensemble predictions of 2009's tropical cyclones initialized with an Ensemble Kalman Filter. *Mon. Wea. Rev.*, **139**, 668 – 688.

Hong, S.-Y., J. Dudhia, and S.-H. Chen, 2004: A revised approach to ice-microphysical processes for the bulk parameterization of cloud and precipitation. *Mon. Wea. Rev.*, **132**, 103 – 120.

Kimball, S. K., 2006: A modeling study of hurricane landfall in a dry environment. *Mon. Wea. Rev.*, **134**, 1901 – 1918.

Noh, Y., W.-G. Cheon, S.-Y. Hong, and S. Raasch, 2003: Improvement of the K-profile model for the planetary boundary layer based on large eddy simulation data. *Bound.-Layer Meteor.*, **107**, 401 – 427.

Rappaport, E. N., and Coauthors, 2009: Advances and challenges at the National Hurricane Center. *Wea. Forecasting,* **24,** 395 – 419.

Reasor, P. D., M. T. Montgomery, and L. D. Grasso, 2004: A new look at the problem of tropical cyclones in vertical shear flow: vortex resiliency. *J. Atmos. Sci.*, **61**, 3 – 22.

Riemer, M., M. T. Montgomery, and M. E. Nicholls, 2010: A new paradigm for intensity modification of tropical cyclones: thermodynamic impact of vertical wind shear on the inflow layer. *Atmos. Chem. Phys.*, **10**, 3163 – 3188.

Rogers, R., S. Chen, J. Tenerelli, and H. Willoughby, 2003: A numerical study of the impact of vertical shear on the distribution of rainfall in Hurricane Bonnie (1998). *Mon. Wea. Rev.*, **131**, 1577 – 1598.

Skamarock, W. C., J. B. Klemp, J. Dudhia, D.O. Gill, D. M. Barker, M. G. Duda, X.-Y. Huang, W. Wang, and J. G. Powers, 2008: A description of the Advanced Research WRF Version 3. NCAR technical note 475+STR, 113 pp.

Simpson, R. H., and H. Riehl, 1958: Mid-troposphere ventilation as a constraint on hurricane development and maintenance. *Proc. Tech. Conf. on Hurricanes,* Miami Beach, FL, Amer. Meteor. Soc., D4.1–D4.10.

Sippel, J. A., S. A. Braun and C.-L. Shie, 2011: Environmental influences on the strength of Tropical Storm Debby (2006). *J. Atmos. Sci.*, **68**, 2557 – 2581.

Sippel, J. A. and F. Zhang, 2010: Factors affecting the predictability of Hurricane Humberto (2007). *J. Atmos. Sci..,* **67,** 1759 – 1778.

Sippel, J. A. and F. Zhang, 2008: A probabilistic analysis of the dynamics and predictability of tropical cyclogenesis. *J. Atmos. Sci.*, **65**, 3440 – 3459.

Whitaker, J.S., T.M. Hamill, X. Wei, Y. Song, and Z. Toth, 2008: Ensemble data assimilation with the NCEP Global Forecast System. *Mon. Wea. Rev.,* **136**, 463–482.

Zehr, R.M., J.A. Knaff**,** and M. DeMaria, 2008: Tropical cyclone environmental vertical wind shear analysis using a microwave sounder. *28th AMS Conference on Hurricanes and Tropical Meteorology*, 28 April-2 May, Orlando, FL.

Zhang F. and D. Tao, 2012: Impacts of vertical wind shear on the predictability of tropical cyclones. *J. Atmos. Sci.*, Submitted.

Zhang F., Y. Weng, Y.-H. Kuo, J. S. Whitaker, and B. Xie, 2010: Predicting Typhoon Morakot's catastrophic rainfall with a convection-permitting mesoscale ensemble system. *Wea. Forecasting,* **25**, 1816–1825.

Zhang F. and J. A. Sippel, 2009: Effects of moist convection on hurricane predictability. *J.*

Atmos. Sci., **66**, 1944–1961.